Pure Appl. Chem., Vol. 80, No. 7, pp. 1365–1379, 2008.
doi:10.1351/pac200880071365

Monodisperse single nanodiamond particulates*

Eiji Ōsawa‡

NanoCarbon Research Institute, AREC, Faculty of Textile Science and Technology, Shinshu University, 3-15-1 Tokita, Ueda, Nagano 386-8567, Japan

Abstract: Detonation nanodiamond (DN) was discovered in 1963, but for several reasons was known only among a small number of scientists until the turn of the century. The most serious cause was the fact that primary nanocarbon particles formed by the "bottom-up method" are in general covalently bound together under high-temperature and -pressure conditions to form large agglutinates, which were difficult to separate by conventional methods. DN was not an exception. A breakthrough led to the isolation of primary particles having the expected size of 4–5 nm by wet-milling with zirconia micro-beads. Thus, long-waited primary particles of DN finally became available in kg quantities in the form of colloidal sol, gel, and readily redispersible flakes. Progress in the development of a new form of the old material is presented.

Keywords: dispersed nanodiamond; agglutination; primary particles; applications; history.

INTRODUCTION

Diamond is considered to be the best all-purpose material with a number of properties ranked as "the highest among known materials on earth", including optical transparency, thermal conductivity, dimensional stability, electric insulation, and chemical stability. A few forms of artificial diamond have been developed for some time. Micron-sized single crystals of diamond have been manufactured since 1955 [1], and their production technology has reached such a level to afford high-quality products at the cost of a few cents per carat. Nevertheless, microdiamonds are exerting themselves only in the backyard, used for polishing and lapping, and the world production has never grown beyond a few hundred tons per year. The reason for the disappointingly modest performance of microdiamonds is simply due to the complete lack of processing capability. Diamond thin films or coatings prepared by chemical vapor deposition (CVD) were expected to perform much better than microdiamond particles with regard to processability, but it has been taking a long time from its beginning in 1954 to identify the developmental direction to the heteroepitaxial synthesis of single-crystalline diamond films by bias-enhanced nucleation and highly oriented diamond growth technique [2]. It will take some more time until macroscopic production of high-quality CVD diamond films, either single-crystalline or polycrystalline, becomes feasible. Finally, diamond-like carbon (DLC) films are attracting more and more attention for the low-friction and chemically inert coating. For DLC films, however, it is difficult to characterize and define atomistic details of structure, and this feature makes this form of diamond unsuitable for scientific research [3].

---

*Paper based on a presentation at the International Conference on Modern Physical Chemistry for Advanced Materials (MPC '07), 26–30 June 2007, Kharkiv, Ukraine. Other presentations are published in this issue, pp. 1365–1630.
‡E-mail: OsawaEiji@aol.com

We would like to introduce here an *almost new* form of diamond, monodisperse single nanodiamond (*mdsn*-D) particles, almost new because these particles have been observed using transmission electron microscopy (TEM) in the past but have never been separated from their agglutinated, aggregated, and agglomerated forms (see below) since their discovery 40 years ago. Our work is still in progress, but we believe *mdsn*-D particles represent a highly potential candidate for a prototypal second-generation nanocarbon [4,5].

BRIEF HISTORY, 1963–2007

Discovery of detonation nanodiamond

One of the popular military explosives, Composition B (40 % TNT + 60 % RDX), is oxygen-deficient, hence upon detonation in an inert medium like argon or water it produces up to 12 % soot by incomplete combustion, which surprisingly contains up to 75 % diamond carbon. This immensely important observation was made in July 1963 by K. V. Volkov, V. V. Danilenko, and V. I. Elin in Snezhinsk, Russia, according to a later paper by Danilenko [6]. According to this paper, at that time at least seven independent research groups (the so-called "diamond club") in the former Soviet Union countries actively engaged in the shock synthesis of diamond, stimulated by the 1961 paper by DeCarli and Jamieson [7] on the phase transition of graphite into diamond upon irradiation with shock wave generated by implosion of Composition B. While trying to reproduce DeCarli's experiments, Danilenko noticed that the yield of diamond sometimes exceeded the amount of starting graphite initially used as the carbon source, and repeated the experiments with less and less graphite to obtain similar trends. Finally, he detonated Composition B without adding graphite but still obtained the diamond-containing soot. He found that unoxidized carbon atoms originally present in explosive molecules crystallized into diamond. In this way, Danilenko achieved a very significant discovery of a unique synthetic method of nanosized diamond, or "detonation nanodiamond" (DN). Unfortunately, apparently due to a defective information system in the previous Soviet army research regime, the discovery was never properly circulated as were the same discoveries made by other members of the diamond club. None of the discoveries were officially archived or published [6].

After Perestroika, the rare event of "multiple discoveries" became known, but no one knew who the first discoverer was. It was on the occasion of the First International Conference on Detonation Nanodiamond held in 2003 in St. Petersburg, Russia, that Danilenko's work was recognized as the first, while those of (late) A. M. Staver's group of Novosibirsk and G. I. Savvakin's group of Kiev succeeded much later, both in 1982. In the Western world, Roy Greiner and his coworkers [8] at Los Alamos observed the same phenomenon in 1988 without knowledge of the activities of Soviet scientists, thus they became the "fourth discoverers".

During this period, another notable incidence occurred that has had lasting and adverse influence on the fate of DN until recently—that is, the overlooking of an extremely tight assembly among primary particles of DN. The discoverers must have applied the well-known technique of determining coherent scattering region by the intensity of X-ray diffraction, and recognized the extremely small size of single-crystalline primary particles, of 4–5 nm, in DN. Later on, TEM observations of the crude products of DN supplied supporting evidence for the size of single crystals in DN. However, we would like to point out that neither of these observations provided information on the special mode of aggregation. Having no way to determine the effective particle size in single-nano range in those days, they interpreted that the grayish powder of DN that they isolated was simple van der Waals aggregates of primary single-crystalline particles, and erroneously named the powder "ultra-disperse diamond" (UDD).

Stagnation

Despite the early and brilliant discovery of DN, Danilenko's group had to suspend work on DN in 1965 for local reasons [6]. While other diamond research groups continued to work, Danilenko's group did not return to DN until almost 20 years later. By that time, however, diamond research in the Soviet Union was classified as top priority, but it was then decided that Soviet scientists should concentrate on the static high-temperature and -pressure method of diamond production, originally developed by the GE group, and abandon further work on the DN research. Thus, there was long stagnation in the development of DN. Fortunately or unfortunately, the discovery of DN did not leak to the Western world, even for a few years after Perestroika in 1989. The fourth discovery by Greiner took place only in 1988 and apparently did not attract much attention among Western scientists. For these reasons, when ex-Soviet scientists were exposed to sudden and severe economic stress by Perestroika, they had enough time to resume the DN research and even develop an industrial production site in Bijsk, Siberia, to make a business out of their own discovery. In this way, the members of the diamond club monopolized the production technology and began exporting UDD. Understandably, however, they could not sell enough UDD and closed down the production site around 1993. The evolution of nanotechnology in 2001 renewed interests in DN and from 2003 we saw small DN factories springing up in Russia, Ukraine, Belarus, and China [6]. However, they produced the same wrong material as before and could not find any major applications.

The reason for the surprisingly long stagnation of 40 years in the development of such a promising material as single nanodiamond particles is the overlooking of effective particle size since the time of discovery. In the past, it has been believed that the primary particles, or crystallites, of DN can be readily reached by ultrasonic dispersion of its conglomerates. However, this premise was not based on the experimental evidence as mentioned below.

Table 1 Chronicle of R&D in DN.

Year	Events	Refs.
1963	Discovery by Volkov, Danilenko, and Elin of DN. Small size of 4–5 nm in primary particles shortly recognized.	[6]
1963–1988	Kept secret within ex-Soviet army regime, research activities suspended.	[6]
Early 1990s	Industrial production began in Russia, Ukraine, and Belarus, but suspended due to poor sales.	[6]
Late 1990s	Production resumed for hard disk finishing steps. China joined production.	[6]
2002	Agglutination of primary particles to form agglutinates of 100–200 in diameter recognized and destroyed by beads-milling to release *mdsn*-D particles.	[9]
2003	First Workshop on DN held in St. Petersburg, Russia.	
2004	NATO Advanced Research Workshop on UNCD held in St. Petersburg, Russia.	[4]
2005	First NEDO International Workshop on Nanocarbon/Nanodiamond held in Hayama, Japan.	
	First paper on *mdsn*-D printed in *Carbon*.	[9]
2006	Second Joint International Symposium on NC/ND held in St. Petersburg, Russia. Sample distribution of *mdsn*-D began.	
2007	A pilot plant for 40 kg/m production of *mdsn*-D completed in Hokkaido, Japan.	
	First paper on the use of *mdsn*-D for seeding in CVD diamond film printed in *Carbon*.	[10]
	First paper on the use of hydrogen of *mdsn*-D for drug carrier printed in *Nano Lett*.	[11]
2008	Third Joint International Symposium on NC/ND to be held in St. Petersburg, Russia.	

First breakthrough (recognition of agglutination)

In 2002–2003, we carried out two series of experiments, hydrothermal reactions and particle-size measurements of commercial NO, which helped us break the long period of stagnation and led us to the first separation of primary particles of DN having the same size as the coherent scattering region observed long ago by X-ray analysis [4,9].

In those days, the primary particles of DN were considered to be accessible readily by sonication, and the primary particle was considered to be surrounded first by a thin layer of spherical graphene shells to give a diamond-nested giant fullerene, which in turn was covered with a partially oxidized layer of amorphous carbons containing metallic impurities and pieces of graphite to make up the outermost surface of primary particles [12]. On the basis of this model, we set out experiments to purify the commercial sample of DN by removing the surface layers of non-diamond carbon atoms by strenuous oxidation. Among a number of oxidation reactions examined, we found treatment with supercritical water at 800 °C and 200 MPa for 24 h the most effective, giving an almost colorless solid and only gaseous reaction products. However, while the graphene shells had disappeared in the TEM image of the solid product, IR and Raman spectra did not substantially change, indicating the persistence of OH groups and large amounts of sp^2-hybridized carbon atoms in some unknown place.

Thereupon, we suspected that there may be domains in the powder of DN where oxidizing agent cannot penetrate. Hence, we went back to the unproven statement that conventional sonication should lead to primary particles. This hypothesis can be verified by measuring the particle size after sonication. Hence, we performed dynamic light scattering (DLS) measurements of the particle-size distribution on a commercial UDD sample before and after supersonic treatments. Before sonication, we observed three peaks at 30–50, 3–5, and 0.2–0.4 μm (Fig. 1a). We assumed, based on the size range alone, that these correspond to agglomerates and secondary and primary aggregates, respectively (Fig. 2). The agglomerates quickly disappeared by pulverization in an agate mortar with concomitant increase in the distribution of secondary aggregates. The latter could be decomposed into primary aggregates by treatments with a 200–400-W laboratory high-power supersonic generator for a short time or with a 100-W sonication washing bath for longer time. However, the distribution of primary aggregates only shifted its center down to 0.1–0.2 μm even after powerful supersonic treatments for longer time and no distribution appeared in the expected single-nano range (Fig. 1b).

These experiments seemed to indicate complex hierarchical agglomeration structure in the commercial DN powder comprising three discrete modes of aggregation, each mode holding component particles by different interparticle force. The forces holding the largest agglomerates must be weak van der Waals forces acting among the secondary aggregates. In turn, the forces acting to hold the secondary aggregates came from van der Waals attraction involving relatively large surface areas of primary aggregates. These two types of aggregation are well known and can be destroyed by grinding and sonication.

Assigning the nature of forces acting to hold constituent particles in the primary aggregates was crucial. As these particles could not be destroyed by intense sonication for prolonged periods of time, forces acting among the constituent particles cannot be the same van der Waals attraction as those acting between coordinatively unsaturated surfaces of larger particles. For this reason, we assume that the constituent particles in the core aggregates are bound by chemical bonding, most likely C–C bonds. We are still unable to identify the inside structure of the primary aggregates, but we simply assume that primary aggregates consist of bonded primary particles, in analogy with the structure of CVD films of ultrananocrystalline diamond (UNCD) [13]. If this assumption proves correct, we should rename the primary aggregate to core agglutinates (Fig. 2). These assignments should be, however, regarded temporary as the DLS particle-size distributions of multipeak systems are not always reliable because of exponential dependence of scattering intensity upon particle size. Moreover, the absence of peaks at 4–5-nm regions does not necessarily exclude the presence of the single nanoparticles, even as the negligibly small scattering from such small particles could readily be overridden by those from the small amounts of aggregates.

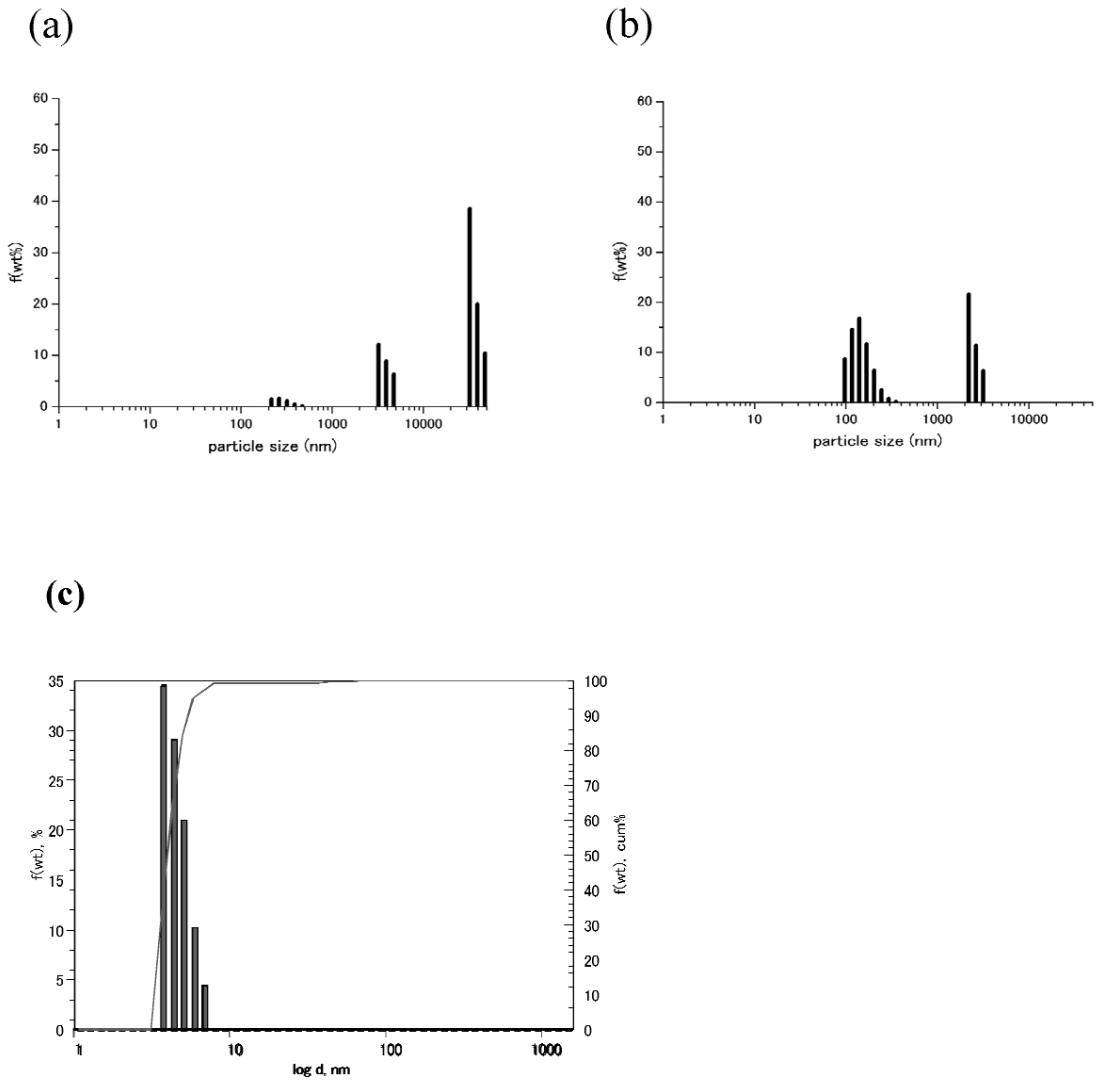

Fig. 1 DLS measurements of particle-size distribution in commercial DN (a) before and (b) after sonication, and (c) after beads-milling. In (c), a broad and extremely weak distribution appear between 35 and 70 nm, but only visible in the graph in the accumulated population graph. This distribution should not be confused with the agglutinate peak in (a) and (b) appearing between 100 and 300 nm. Solvent is water.

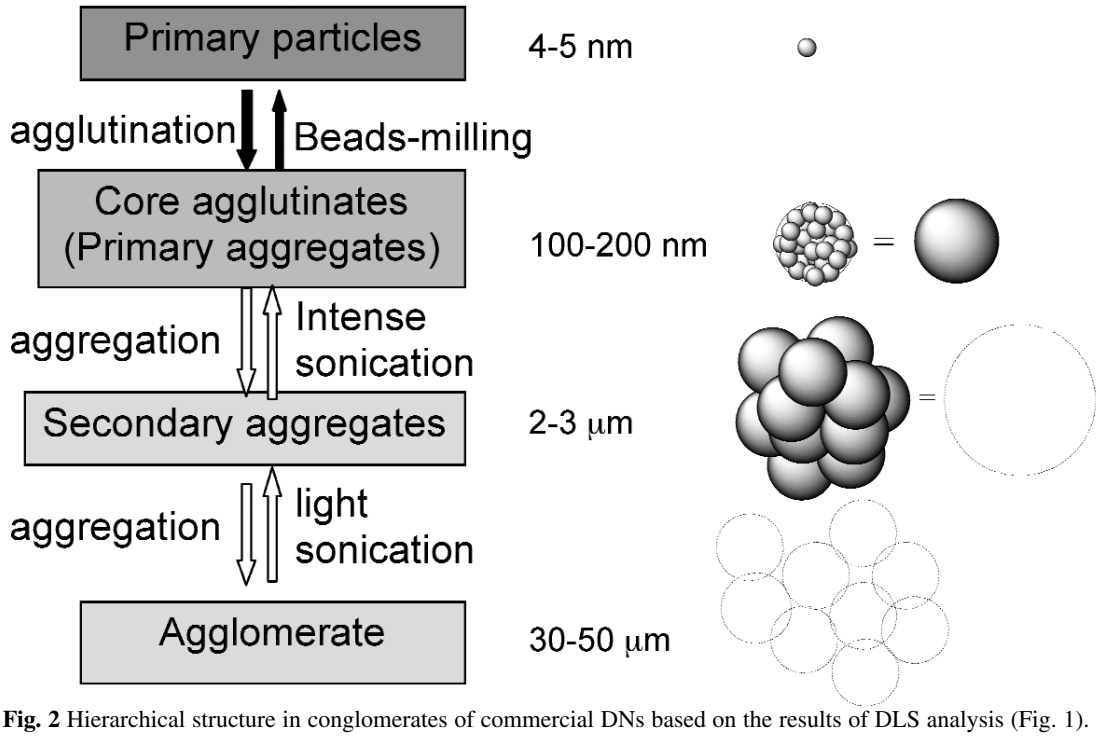

Fig. 2 Hierarchical structure in conglomerates of commercial DNs based on the results of DLS analysis (Fig. 1).

The most important conclusion from these experiments is the recognition of core agglutinates with 100–200 nm in size and the unusually tight binding within the agglutinates. We later confirmed that even one of the most powerful sonicators available (2 kW) failed to decompose core aggregates into primary particles of DN. The spherical shape of the core agglutinates as seen in their SEM pictures taken by Vul's group [14] as well as the normal mode of particle size distribution (Figs. 1a,b) suggests that the core agglutinate particles have undergone a sort of thermal equilibrium. It is likely that, when the diamond crystallites (grain) formed in the high-temperature and -pressure domain of shock wave stopped growing as the wave front moved out of the reaction zone, grains stay at high temperature for short time and combine with each other to form a sort of polycrystalline mass wherein primary particles are bound by multitudes of C–C covalent bonds with the neighboring particles. If this picture is correct, we need to cleave the C–C bonds in the grain boundaries in order to free primary particles (Fig. 3).

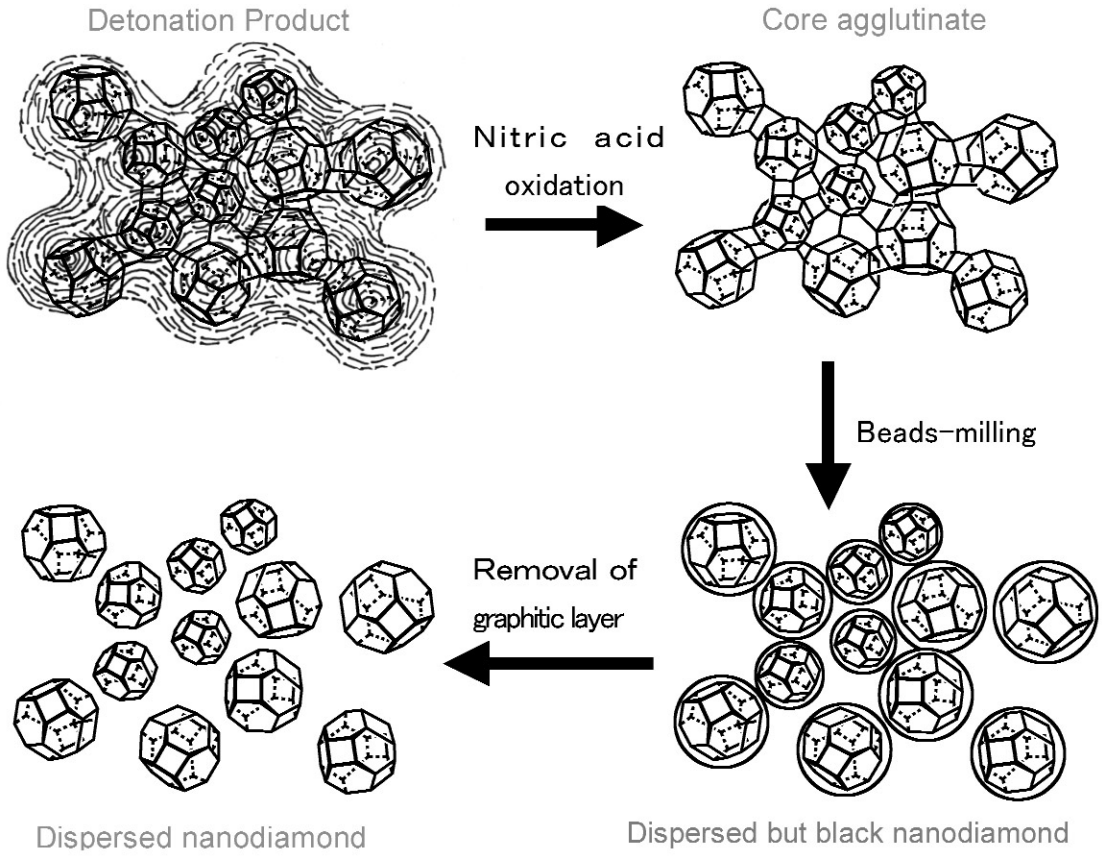

Fig. 3 Illustrations of complex transformation occurring on a core agglutinate during the purification process of detonation synthesis of nanodiamond. Core agglutinate (upper right) may contain graphitic fragments in the grain boundary region, kept intact during nitric acid oxidation. However, we think the beads-milling process produces graphitic carbons by converting some of the carbon atoms on the surface of primary particles into graphitic patches as the primary particles are exposed to the impact of beads. Work on the final step to remove the graphitic shell is still in progress. Fragmented hatch (in upper left drawing) means soot, truncated octahedra means particles, and circles (lower right) mean partial graphitic layers.

Second breakthrough (beads-milling)

As can be readily anticipated, the disintegration of core agglutinates must be a highly energetic process, to breaking up a large number of C–C covalent bonds in the grain boundaries. It would be advisable to perform the disintegration in wet media in order to annihilate free radicals formed at the bond-cleavage sites. Fortunately, we succeeded in solving these problems by applying wet-milling with micron-sized beads [9]. This variant of milling is a relatively new technique developed within powder technology and was almost totally unknown to chemical laboratories. The technique is useful not only for disintegrating tight agglutinates but also for future application of mechanical alloying to nanoscience/technology [15]. For these reasons, we discuss this technique in some depth below.

In the ball-milling, a heavy ball falling from the ceiling of a rotating mill crushes substrate material with surprisingly high efficiency. Efficiency is high because the large kinetic energy of the falling ball (caused by high density of ceramic or iron ball) is released at a small area of contact with the inner wall of the mill, where a small amount of substrate is always present and receives the full impact of a whole ball. The final size of substrate particles depends primarily on the contact area of the ball with

the wall, which in turn is determined by Young's modulus and the surface curvature of ball. For a fixed ball material (e.g., high-density ceramics such as silica and zirconia), higher curvature and smaller contact area can be obtained by decreasing the diameter of the ball. As smaller and smaller balls, or beads, are used as the crusher to obtain finer powders, the potential energy of a lighter ball decreases and becomes insufficient for crushing. Therefore, the energy must be supplemented by giving higher kinetic energy. For this reason, the crushing media need to be rotated at high speed in the beads-milling. For this reason, this method is also called stirred-media or attrition milling (Fig. 4).

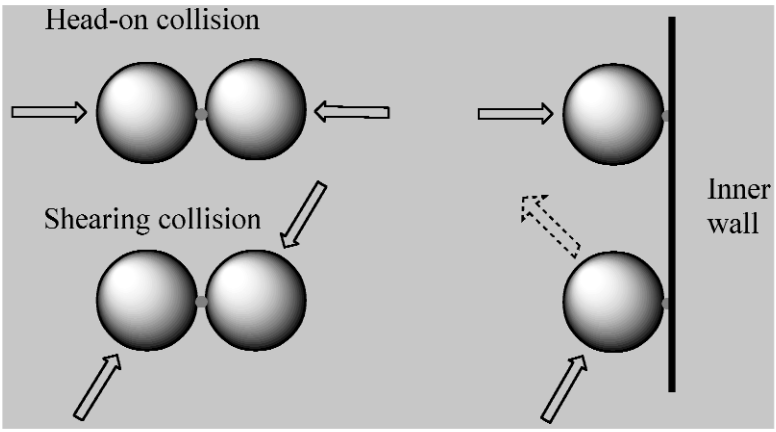

Fig. 4 Mechanism of beads-milling. In the case of crushing crude product of DN (secondary aggregates or core agglutinates, gray spots), heavy and hard zirconia beads (sphere) is packed to fill much of the mill space and rotated at high speed. The impact of colliding beads upon the pinched substrate particles should be enormous. As the milling proceeds to release more and more primary diamond particles, more and more primary diamond particles are directly exposed to the impact of collision. The diamond-zirconia collisions lead to (1) scraping of beads material which contaminates diamond product, and (2) conversion of surface diamond atoms into graphitic patches as the major consequences.

In practice, we used a commercial vertical beads-mill (Ultra Apex Mill UAM-015, equipped with a 160-ml mill, made from zirconia-plated SUS, manufactured by Kotobuki Eng. & Manuf. Co., Tokyo), in which yttrium-stabilized zirconia beads having an average diameter of 30 μm (manufactured by Toso Co., Tokyo) are packed to the extent of 70–80 % of the mill volume, leaving 30–20 % space to fill with 10 % aqueous suspension of core agglutinates, which is circulated through the mill by using a peristaltic tube pump. Using this set-up, we succeeded in disintegrating core agglutinates into their grains, namely, the long-waited primary particles of *mdsn*-D. In addition to the high packing rate of beads in the mill, there are a number of conditions to be adjusted, including the type and size of beads, rate of agitation, concentration, and rate of circulating suspension of agglutinates, choice of solvent, and temperature. Some of the conditions have been optimized, and it is possible at present to process 50 g of agglutinates to primary particles in two hours of beads-milling. While the progress of disintegration can be monitored by sampling aliquots and measuring particle sizes by DLS measurements, it can also be noticed by development of dark coloration and transparency in the circulating suspension. At the end of operation, the initial suspension of the gray powder changed itself into clear but pitch-black colloidal solution. Black color is actually a result of an undesirable side reaction. We have some spectroscopic evidence to indicate the formation of graphitic patches on the surface of the primary particle by diamond-graphite transformation caused by the impact of shearing collision with beads [16–18]. We will come back to the black coloration problem below.

After removing small amounts of coarse grains that remained uncrushed by filtration and centrifugation, the colloidal solution of *mdsn*-D particles turned out to be surprisingly stable, giving no pre-

cipitates for months. DLS analysis of typical colloidal solution thus obtained is shown in Fig. 1c, showing 99.4 wt % of single nanoparticles of 4.6 ± 0.8 nm in diameter. When left standing in concentrations higher than about 8 %, the solution quickly solidifies to a soft gel, but can be readily turned back to smooth sol by adding small amounts of water [19]. Evaporation of water gave needle-shaped heavy and dark flakes. As expected, the behaviors of *mdsn*-D are completely different from those of agglutinates as mentioned below.

CHARACTERISTICS OF *mdsn*-D PARTICLES

To our knowledge, *mdsn*-D is the first example of nanocarbon species that is mass-producible, stable, potentially useful, and typically single-nano in size, thus providing the first nanocarbon particle with which we should be able to study fundamental behaviors of nanoparticles. Whereas C_{60} was isolated before *mdsn*-D and well studied, it is too small to be a standard nanoparticle, even soluble in organic solvents, and can be purified by recrystallization and other known purification methods to 100 % purity level. All these features are missing in typical nanoparticles. In this respect, C_{60} still belongs to traditional objects of chemistry rather than a nanoparticle. In contrast, *mdsn*-D is absolutely insoluble in any organic solvents, nonsubliminal, nonvolatile, nonmelting, and, in short, nonpurifiable by any of the purification methods known for usual molecules. These are typical behaviors of nanoparticles. Here we also emphasize contrasting behaviors of *mdsn*-D compared to its agglutinated counterpart, "UDD" (Table 2).

Table 2 Comparison between core agglutinate ("UDD") and primary particle (*mdsn*-D) of DN.

	Core agglutinate ("UDD")	Primary particle (*mdsn*-D)
No. of grain	70 000 ~ 350 000	1
Size, nm	60–200	4–5
Colloidal solution	Unstable, precipitates, turbid, gray, no gel formation	Stable, no precipitates, transparent, black, gel formation from 10 %
DSC of aq. gel	No remarkable feature	Nonfreezing water layer
TGA	No remarkable feature	Explosive combustion at ca. 500 °C
Raman	D > G	D >> G
SEM/TEM	Visible/assembly	Invisible/dispersed

We wish to remove impurities from *mdsn*-D and increase the content of diamond carbon atoms as much as possible to obtain a standard sample of *mdsn*-D, with which we could determine physical constants of *mdsn*-D species. However, we are still working toward this goal. We started purification work a few years ago, attempting first of all to remove the black color of the colloid. There can be several reasons for nanodiamond particles acquiring black color. Natural diamonds often look dark to black due to the tiny metallic impurities in the inside of crystal lattice which scatter incident light efficiently. In that case, it would be meaningless to remove the color as we have to destroy the whole crystal. CVD diamond films consisting of so-called UNCD grains often carry pale to dark brown color due to the presence of impurities, especially graphitic, in the large volume of grain boundaries. For UDD, it has often been suggested that fullerene-like graphene layers surround the surface [12]. Shames and Panich observed, in high-power decoupling (HPDEC) ^{13}C MAS NMR spectra of both UDD agglutinates and *mdsn*-D, a sharp sp^2-C signal at $\delta = 111$ ppm, which indicates the presence of graphene-layered structures with "decent perfection" [16].

It is likely that the dark coloration in CVD/UNCD, UDD, and *mdsn*-D originates from common graphene impurities. In CVD/UNCD, the presence of graphene pieces in grain boundaries are well anticipated and studied [20]. In UDD, highly crystalline graphitic layers could have been formed when it moved from the diamond-stable region into the graphite-stable region in the phase diagram of carbon

in the detonation chamber, but at this time, core agglutinates must have been formed according to our hypothesis, hence the concentration of graphene layers are small and almost invisible. In *mdsn*-D, much larger amounts of graphene patches must be generated and crystallized by the pinning effect during the milling on the exposed surface of primary particles to give intense black color [18].

We have applied a number of known methods to remove the graphitic layers considered to cover the surface of *mdsn*-D particles, but have not yet succeeded at the time of writing this paper. High order in the graphitic structure may be one reason for slow reaction. Therefore, we are still not in a position to determine the standard physical constants of *mdsn*-D particles. More or less qualitative pictures of the properties and behaviors of black *mdsn*-D are summarized below (Table 3).

Table 3 Properties of *mdsn*-D particles.

Item	Description	Refs.
Physical const.	Not yet determined due to lack of standard sample	
Elemenatry analysis	Impossible due to high hygroscopicity	
Hydration	In aqueous gel, nonfreezing layer of water surrounds the surface with a thickness of about 1 nm.	[21]
Shape	Irregular and spherical polyhedra probably relating defective truncated octahedra	
Diameter, nm	4.5 ± 0.5 (coherent scattering region) 4.6 ± 0.8 (DLS)	[19,22]
Self-organization	High. Upon removal of water from aqueous colloid, gelation starts at about 8 wt %. At concentrations above 20 %, self-organized to shapes like ribbon-like films, fine rod-like flakes and whiskers. Freeze drying often leads to fine needles or extremely long whiskers longer than 1 cm.	[23]
Color	Flakes are colored brown to black, while colloidal solution looks deep black in concentrations higher than 1 %, but deep to pale brown at concentrations lower than 0.2 %. Colors are considered to arise from partial graphitic patches on the surface.	[16]
Fluorescence	650 nm, weak but intensifies upon bombarding with nitrogen ions	
IR, cm^{-1}	3430(vs, ν_{OH}), 2925(sh, ν_{CH}), 1708(s, $\nu_{C=O}$), 1631(s, δ_{OH}), 1500–1000 (br) with peaks at 1363 and 1228	[4]
^{13}C MAS NMR, ppm	34–35 (diamond, sp^3C), 111 (graphitic, sp^2C), intensity ratio 8.8 :1	[16]
Aggregation	Very strong upon thorough drying to give solids difficult to redisperse. Colloid solutions and gels are stable and do not produce precipitates after long standing.	
Stable region of aq. colloid	pH 3~6, ζ-potential +40~+50, maximum ζ-potential of +53 mV occurs at pH 4.88	[24]
Good media for colloidal solution	Water, DMSO, EtOH, ethylene glycol, 1-methyl-2-pyrrolidinone, 2-methoxyethanol	[24]
Biocompatibility	Cell toxicity none, genetic toxicity under examination	[25–27]

Size, shape, and modeling

We adopt here 4.5 ± 0.5 nm as a representative size for *mdsn*-D obtained by using small-angle X-ray scattering [12]. This average size is more reliable than the values obtained by DLS alone, but the latter values more or less correspond to this one, including small standard deviation. For example, we recently obtained an average value of 4.6 ± 0.8 nm from systematic DLS measurements of a well-milled sample containing 99.4 wt % of this peak for a wide range of sample concentrations [19]. The narrow size distribution of primary particles is one of the remarkable assets of *mdsn*-D.

Shapes are more difficult to determine than size. TEM has so far revealed only limited information on the shape. In some images, edges, apexes, and even facets could be identified, albeit only inconclusively (Fig. 5). The most likely shapes are defective and irregular modifications of truncated octahedron or cuboctahedrane. All the theoretical calculations and simulations of nanodiamond have been performed on truncated octahedron. Our preliminary MM3/AM1 geometry optimization of variously sized truncated octahedral with partial hydrogen termination on the triangular (111) facets but unterminated on the square (100) facets gave the following numbers for a typical model: diameter = 4.28 nm, MW ≈ 62 000, surface atoms = 810, internal atoms = 4296, total atoms = 5106, secondary C atoms in square facet = 486, tertiary C atoms in triangle facet = 324, surface atoms/total atoms = 15.9 %. No full-scale modeling calculation including electronic states has been performed as yet but these numbers help the imaging of the skeletal structure of average primary particles of *mdsn*-D.

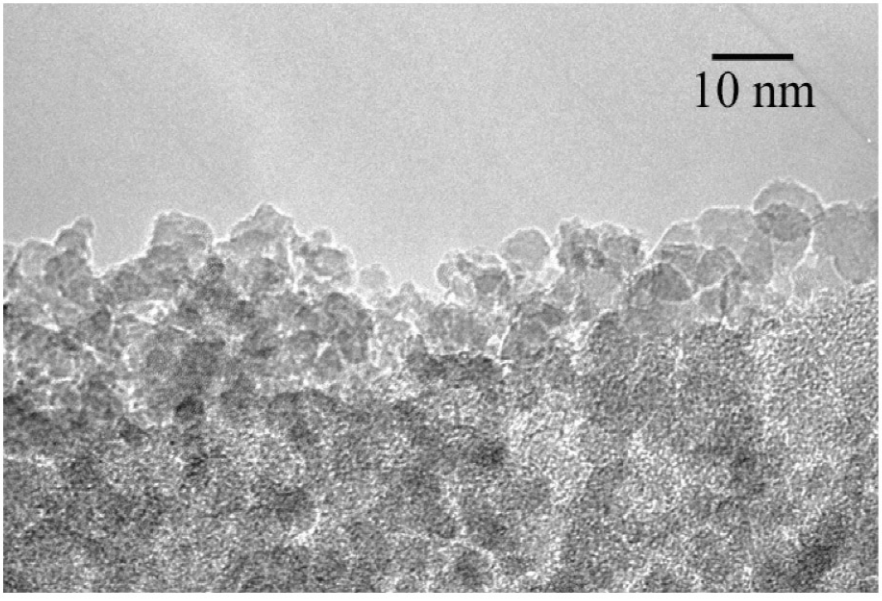

Fig. 5 TEM image of *mdsn*-D particles, reaggregated upon drying.

Surface properties

The high surface/total atomic ratio, large surface area expected for monodispersed state, and pronounced surface activity caused by high curvature of single-nano sphere all combine to predict remarkably active surface in *mdsn*-D particles. Behaviors of *mdsn*-D particles mentioned above already revealed remarkably high tendency to aggregate, ready diamond-graphite phase transition on the surface, great hygroscopicity (Table 3), and explosive combustion upon heating in air at relatively low temperature (Table 2). Gel formation from aqueous colloid of relatively low concentration (ca. 8 %) suggests strong hydration inducing hydrogen-bond network in bulk water. An illustrative evidence for

strong hydration on the particle surface was obtained while performing differential scanning calorimetry (DSC) on 50 % aqueous gel: a significant nonfreezing endothermic peak at –8 °C in addition to the freezing peak of bulk water at 0 °C (Fig. 6). Analysis of Fig. 6A indicated the following facts:

- Only single nanoparticles form a nonfreezing layer of water.
- A *mdsn*-D particle attracts water about one-half its own weight to its surface.
- Molar heat of nanophase water (3.1 kJ/mol) is about one-half that of bulk water (6.0 kJ/mol), thus indicating strong orientation of water molecules toward the particle surface.
- The thickness of nonfreezing water layer is about 1 nm [21].

These results indicate highly polar nature of the particle surface. The polarity is supposed to come from oxygen-containing functional groups, especially carboxyl groups as confirmed by preliminary titration with $NaHCO_3$, C–H groups, and sp^2(graphite)–sp^3(diamond) interface, all known to be present on the surface of *mdsn*-D particles. If oxygen atoms in water molecules are the counterpart of electrostatic interaction between these polar groups and water, then protons with partial positive charge will be directed to the outside in the nonfreezing hydration shell.

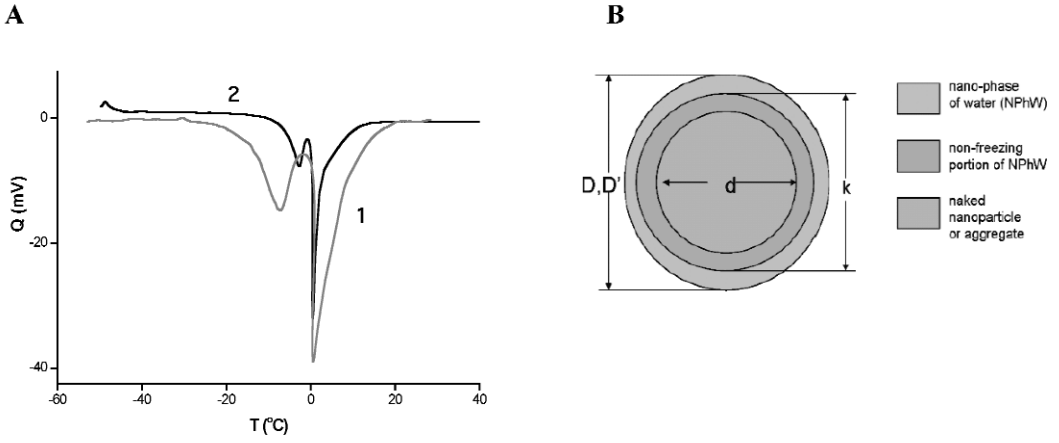

Fig. 6 Nonfreezing water layer absorbed on the surface of *mdsn*-D particle. (A). Typical DSC scans: (1) aqueous gel of *mdsn*-D particles, total amount of water, M_{H2O} = 10.1 mg, mass of *mdsn*-D, M_C = 10.2 mg, (2) aqueous gel of C_{60} cluster, total amount of water, M_{H2O} = 2.7 mg, mass of fullerene C_{60}, M_C = 2.0 mg. (B). Core-shell model of nanophase water (nonfreezing layer of water) around the nanodiamond particle.

Stability of colloid

One of the biggest surprises that we encountered so far is the unexpectedly high stability of colloidal particles of *mdsn*-D in water, and also in some organic solvents like alcohols and dimethyl sulfoxide. If it were not for this feature, beads-milling in water would have been impossible to carry out and the primary particles of *mdsn*-D never separated. The colloidal stability seems to have originated from the surface polarity mentioned above. Other novel features of *mdsn*-D particles, such as a high tendency toward self-organization, leading to spontaneous formation of whiskers, films, and fibers of nanodiamond from its colloid, and hydrogel formation, may be all related with localized polarity on the surface. The polarity may be changed and controlled by chemical modification or reconstruction of surface as clear colloidal solution may be subjected to homogeneous reactions.

Nontoxicity

Like any other nanospecies, nanodiamond should be subjected to critical evaluation of all kinds of health risk possibilities by qualified scientists. A complete absence of cytotoxicity in *mdsn*-D has been reported (Table 3).

APPLICATIONS

The surface polarity of *mdsn*-D particles not only caused a few novel properties and behaviors to appear, but also attracted the interests from other scientists and researchers to study applicative possibilities of *mdsn*-D even at the present, by no means in a satisfactory level of purification (Table 4). The high potential of *mdsn*-D particles is clearly visible. Among a number of preliminary tests listed in this table, drug delivery and its slow release by hydrogel is a big surprise [11]. No less interesting is the progress in using colloidal solution of *mdsn*-D for seeding of homoepitaxial growth of CVD polycrystalline diamond film [10]. Uniformity and surface smoothness of ultra-thin diamond film obtained by the initial attempts are very good [20].

Table 4 Partial list of promising applications of *mdsn*-D particles.

Form	Field	Example	Note (refs.)
Dispersed particles	Superfine/high-speed polishing	High-speed chemical-mechanical polishing	Good results obtained in preliminary stages
	Lubrication	Low-friction joints of all kinds	Positive effects confirmed repeatedly. Intensive work going on.
	Strengthening agent for composites	Matrices: metals, alloys, plastics, synthetic polymers, glass, ceramics	Preliminary tests performed for Cu and W by using mechanical milling [28]
	Electron-emitting cathode	Not studied yet	
	Seeds for homoepitaxial growth of CVD polycrystal diamond	Heat spreader for electronic devices, low-friction coating	Preliminary tests under way. Results are quite promising [1,10].
	Fluorescence emitter	Cell imaging	Preliminary tests under way. Results are promising [29].
	Catalyst carriers	Not studied yet	
	Cell therapy	Not studied yet	
	Surface derivatives	Perfluoro-ND (nanobearings)	Pursued by a Japanese company
	Solid-phase transition	Spherical nanographite (solar energy storage)	Preliminary testing being planned
Gel	Drug carrier	Cancer therapy	In progress, highly promising [11]
	Transportation and storage	Stable dispersion systems	Being used for transportation
Assemblies	Powder metallurgy	Heat spreader for electronic devices	No example of success yet
	Multilayered coatings	Biocompatible medical	In progress, highly promising composites

One large area of application open for many materials scientists is to use our particles as a reinforcing component for a variety of known materials. In this case, the diamond–graphite transition must be avoided by keeping molding temperature below about 800 °C. However, a couple of very important and fundamental techniques are still missing, namely, the methods of dispersing and measuring distribution of the single nanoparticles in solid matrices. For the former, we proposed nano/nano dis-

persion principle [28], but for the latter, we have at the moment only the primitive dielectric spectroscopy in mind. One more interesting property of *mdsn*-D is its lubricating ability in aqueous dispersion.

PERSPECTIVES

We feel that *mdsn*-D particles, the oldest known material in new attire, have begun to demonstrate a latent capability for becoming one of the major materials for nanotechnology. We are still concerned with molding the *mdsn*-D particles by powder metallurgy into any desired shapes, thereby realizing a general-purpose material. One of our dreams is "diamond glasses", namely, glasses dispersed and reinforced with *mdsn*-D particles that can transmit more light than glass and withstand earthquakes of high magnitudes when used as building materials. We also have good perspectives in developing the notable tendency for *mdsn*-D particles to self-organize, into sophisticated and diversified applications.

There are a few other requirements for a new material to be produced and applied on a large scale, including cost and supply of raw materials. Good progress is also being made on these features, but they will be discussed elsewhere.

ACKNOWLEDGMENTS

I thank all the collaborators and friends who contributed to a work described herein. Some of the names appear in references. This work was partially supported by NEDO International Cooperative Grant No. 2004IT081.

REFERENCES

1. R. M. Hazen. *The Diamond Makers*, Cambridge University Press, Cambridge (1999).
2. K. Kobashi. *Diamond Films, Chemical Vapor Deposition for Oriented and Heteroepitaxial Growth*, Elsevier, Oxford (2005).
3. C. Donnet, A. Erdemir. *Tribology of Diamond-like Carbon Films: Fundamentals and Applications*, Springer, Berlin (2007).
4. E. Ōsawa. In *Synthesis, Properties and Applications of Ultrananocrystalline Diamond*, D. Gruen, A. Ya. Vul', O. Shenderova (Eds.), pp. 231–240, Springer, Dortrecht (2005).
5. E. Ōsawa. *Diamond Relat. Mater*. **16**, 2018 (2007).
6. V. V. Danilenko. *Phys. Solid State* **46**, 595 (2004).
7. P. S. DiCarli, J. C. Jamieson. *Science* **133**, 1821 (1961).
8. N. R. Greiner, D. S. Phillips, J. D. Johnson, F. Volk. *Nature* **333**, 440 (1988).
9. A. Krüger, F. Kataoka, M. Ozawa, A. Aksenskii, A. Ya. Vul', Y. Fjino, A. Suzuki, E. Ōsawa. *Carbon* **43**, 1722 (2005).
10. O. A. Williams, O. Douheret, M. Daenen, K. Haenen, E. Ōsawa, M. Takahashi. *Chem. Phys. Lett*. **445**, 255 (2007).
11. H. Huang, E. Pierstorff, E. Ōsawa, D. Ho. *Nano Lett*. **7**, 3305 (2007).
12. A. E. Aleksenskii, M. V. Baidakova, A. Ya. Vul', V. I. Siklitskii. *Phys. Solid State* **41**, 668 (1999).
13. D. M. Gruen. *MRS Bull*. **10**, 771 (2001).
14. A. Y. Vul', E. D. Eydelman, M. Inakuma, E. Ōsawa. *Diamond Relat. Mater.* **16**, 2023 (2007).
15. E. Oda, K. Ameyama, S. Yamaguchi. *Mater. Sci. Forum* **503–504**, 573 (2006).
16. A. M. Panich, A. I. Shames, H.-M. Vieth, M. Takahashi, E. Ōsawa, A. Ya. Vul', A. Ya. *Eur. J. Phys. B* **52**, 397 (2006).
17. A. I. Shames, A. M. Panich, S. Porro, M. Rovere, S. Musso, A. Tagliaferro, M. V. Baidakova, V. Yu. Osipov, A. Ya. Vul', T. Enoki, M. Takahashi, E. Ōsawa, O. A. Williams, P. Bruno, D. M. Gruen. *Diamond Relat. Mater.* **16**, 1806 (2007).

18. E. D. Eidelman, V. I. Siklitsky, L. V. Sharonova, M. A. Yagovkina, A. Ya. Vul', M. Takahashi, M. Inakuma, E. Ōsawa. *Diamond Relat. Mater*. **14**, 1765 (2005).
19. E. Ōsawa. *NCRI Tech. Bull*., No. 3, 1–6 (2007) (see <http://nano-carbon.com>).
20. O. A. Williams, M. Nesladek, M. Daenen, S. Michaelson, O. Ternyak, A. Hoffman, E. Ōsawa, K. Haenen, R. B. Jackman, D. M. Gruen. *Diamond Relat. Mater.* (2008). In press.
21. M. V. Korobov, N. V. Avramenko, A. G. Bogachev, N. V. Rozhkova, E. Ōsawa. *J. Phys. Chem. C* **111**, 7330 (2007).
22. A. E. Aleksenskii, M. V. Baidakova, A. Y. Vul', V. Y. Davydov, A. Pevtsova. *Phys. Solid State* **39**, 1007 (1997).
23. H. Huang, L. Dai, E. Ōsawa. Unpublished results.
24. M. Ozawa, M. Inakuma, M. Takahashi, F. Kataoka, A. Krüger, E. Ōsawa. *Adv. Mater*. **19**, 1201 (2007).
25. A. M. Schrand, R. C. Murdock, E. Ōsawa, J. J. Schlager, S. M. Hussain, L. Dai. *Diamond Relat. Mater.* **16**, 2118 (2007).
26. A. M. Schrand, H. Huang, C. Carlson, J. J. Schlager, E. Ōsawa, S. M. Hussain, L. Dai. *J. Phys. Chem. B* **111**, 2 (2007).
27. A. M. Schrand, J. Johnson, L. Dai, S. M. Hussain, J. J. Schlager, L. Zhu, Y. Hong, E. Ōsawa. In *Safety of Nanoparticles: From Manufacturing to Clinical Applications*, T. Webster (Ed.), Springer, Berlin. In press.
28. V. Livramento, J. B. Correia, N. Shohoji, E. Ōsawa. *Diamond Relat. Mater*. **6**, 202 (2007).
29. Y. Colpin, A. Swan, A. V. Zvyagin, T. Plakhotnik. *Opt. Lett*. **31**, 625 (2006).